
Recognizing object affordances to support scene reasoning for manipulation tasks

Fu-Jen Chu¹, Ruinian Xu¹, Chao Tang¹ and Patricio A. Vela¹

Abstract

Affordance information about a scene provides important clues as to what actions may be executed in pursuit of meeting a specified goal state. Thus, integrating affordance-based reasoning into symbolic action planning pipelines would enhance the flexibility of robot manipulation. Unfortunately, the top performing affordance recognition methods use object category priors to boost the accuracy of affordance detection and segmentation. Object priors limit generalization to unknown object categories. This paper describes an affordance recognition pipeline based on a category-agnostic region proposal network for proposing instance regions of an image across categories. To guide affordance learning in the absence of category priors, the training process includes the auxiliary task of explicitly inferencing existing affordances within a proposal. Secondly, a self-attention mechanism trained to interpret each proposal learns to capture rich contextual dependencies through the region. Visual benchmarking shows that the trained network, called *AffContext*, reduces the performance gap between object-agnostic and object-informed affordance recognition. *AffContext* is linked to the Planning Domain Definition Language (PDDL) with an augmented state keeper for action planning across temporally spaced goal-oriented tasks. Manipulation experiments show that *AffContext* can successfully parse scene content to seed a symbolic planner problem specification, whose execution completes the target task. Additionally, task-oriented grasping for cutting and pounding actions demonstrate the exploitation of multiple affordances for a given object to complete specified tasks.

Keywords

Recognition, Manipulation Planning, Grasping, AI Reasoning Methods

Introduction

Identifying the functionalities, or *affordances*, of object parts aids task completion by informing robot manipulators on how to use or interact with an object. Adult humans possess rich prior knowledge for recognizing affordances of object parts. The affordance knowledge supports identification of potential interactions with nearby objects, and contributes to planning manipulation sequences with these objects towards achievement of a defined task. Endowing a robot with the same capabilities is crucial for assistive robots operating in human environments on a daily basis.

Affordance detection of object parts in images is frequently cast as a segmentation problem (Myers et al. 2015; Srikantha and Gall 2016; Nguyen et al. 2016a; Roy and Todorovic 2016; Nguyen et al. 2017; Do et al. 2018). Object parts sharing the same functionality are segmented and grouped at the pixel level, then assigned the corresponding affordance label. This problem formulation permits the use of state-of-the-art semantic segmentation architectures based on convolutional neural networks (CNNs) derived by the computer vision community (Krizhevsky et al. 2012). However, affordance identification differs from conventional semantic segmentation based on visual cues or physical properties, and need not require assigning labels to all image pixels. Understanding functionalities of an object part requires learning the concept of potential interactions with or use by humans. State-of-the-art affordance detection

architectures (Nguyen et al. 2017; Do et al. 2018) improve segmentation performance by jointly optimizing for object detection and affordance prediction. The object prior and instance features inferred from the detection process improve pixel-wise affordance map predictions. Given that per-object bounding box and per-pixel label annotations are labor-intensive, existing affordance datasets contain few object categories when compared to commonly seen classification datasets (Krizhevsky 2009; Deng et al. 2009; Krasin et al. 2016) in the vision community. Consequently, a limited amount of object categories can be learned with these datasets, while the open-world involves more diverse categories. In effect, the specificity of object priors limits generalizability.

Generalizing learnt affordances across novel object categories is essential for open-world affordance recognition and would more fully utilize affordance annotated datasets. Decoupling the object category prior from the instance feature space performing affordance prediction removes

¹School of Electrical and Computer Engineering, Georgia Institute of Technology, GA, USA.

Corresponding author:

Fu-Jen Chu, Intelligent Vision and Automation Laboratory (IVALab), School of Electrical and Computer Engineering, Georgia Institute of Technology, North Ave NW, Atlanta, GA 30332.

Email: fujenchu@gatech.edu

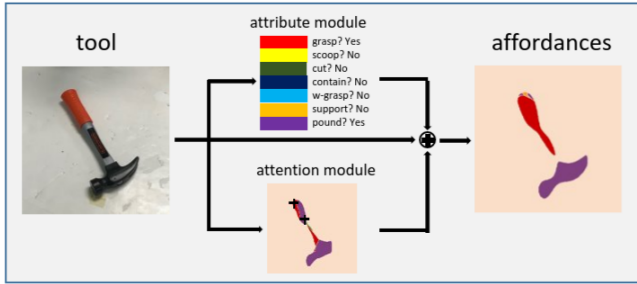


Figure 1. Affordance detection framework with the proposed attribute and attention modules. The attribute and attention modules improve pixel-wise prediction of object part affordances. The attribute module (upper branch) predicts affordances for a region of interest as shareable attributes across categories. As an auxiliary task, it guides the local region feature learning. The attention module (bottom branch) learns dependencies across pixels. For example, the two *plus marks* on the hammer’s handle with high correlation should have the same predicted affordance labels.

the specificity. It also undermines affordance estimation since affordances are typically associated to object parts. Replacing the object category detection process with an *objectness* detection branch parallel to the affordance segmentation bridges the gap for novel categories while maintaining the benefits of utilizing local features for predicting object part affordances, but incurs a performance drop (Chu et al. 2019a). When the internal feature space does not exhibit the richness or performance needed, one means to compensate for information loss in the network is to incorporate attention mechanisms (Vaswani et al. 2017), in particular attention for image-level segmentation tasks (Yuan and Wang 2018; Zhang et al. 2018; Fu et al. 2019).

Our prior work (Chu et al. 2019a) described a category-agnostic affordance detection architecture with a parallel *objectness* detection branch, which could be interpreted as an instance-based attention module. With instance features agnostic to object label, the segmentation branch training process implicitly learns features attuned to pixel-level affordances for each object proposal. The generalized approach sacrifices performance and exhibits an affordance segmentation score drop of 20% relative to object-aware approaches. To mitigate the performance drop, we explore the addition of an intra-region processing module to learn long-range or non-local affordance relationships across instance contexts. In affordance prediction networks, this type of attention module supports high-level understanding by capturing correlations between affordances and other appearance cues (such as object form). Internalizing these correlations improves segmentation accuracy. Furthermore, affordances are shared across the object parts of different objects with similar functions (and possibly similar forms). Thus seen or known affordances may be present in unseen or novel object categories observed in the open-world. To learn visual cues indicative of function, affordances are also used as object attributes shared across object categories in the *objectness* branch. In lieu of strong object priors from an object detector, affordance attribute recognition serves to guide the object instance regions to learn shareable features across novel object categories. Fig. 1 illustrates the general concept of the proposed

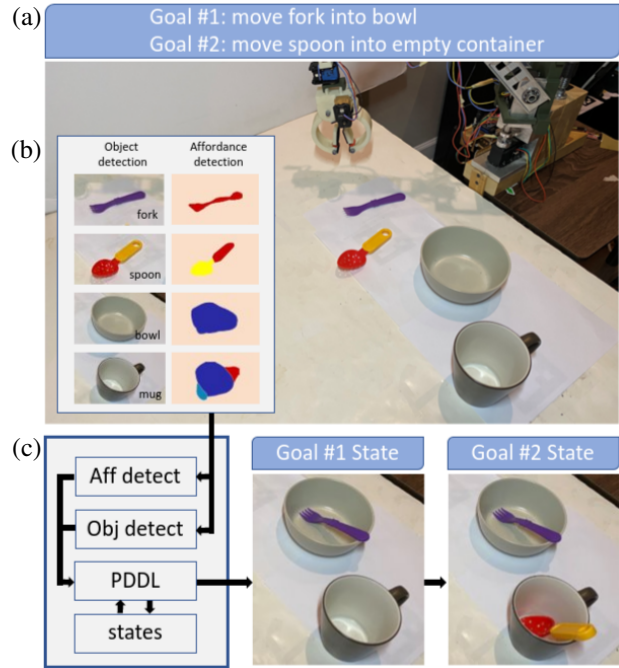


Figure 2. Illustration of the agnostic affordance detection framework with PDDL for goal-directed physical robotic manipulations. **(a)** The overall goal is to first move the fork into the bowl, and then move the spoon into the mug. *Goal #1* explicitly specifies the object to grasp (fork), and the object to contain (bowl). *Goal #2*, however, requires knowledge from previously achieved goal state; **(b)** The proposed category-agnostic affordance detector predicts possible actions to be performed on object parts. Together with a pre-trained object detector, both objects and affordances in the robot’s view are identified; **(c)** Given a goal state, detected objects and affordances form the initial state for PDDL to plan an action sequence for execution. Given a second goal state, the previous goal state contributes to current initial state for PDDL to inference and plan.

affordance detection modules with attention and attribute learning. For a given object region proposal, the *objectness* detection branch leverages affordance attributes to enhance detection via affordance context. Likewise, the segmentation branch leverages attention to promote improved awareness of affordances within an image region proposal. The approach, called *AffContext*, reduces the existing performance gap and supports specification based manipulation using a basic manipulation grammar with affordance-informed predicates.

For planning with affordances, our earlier work (Chu et al. 2019a) defined a symbolic reasoning framework with Planning Domain Definition Language (PDDL) (McDermott et al. 1998) for achieving simple goal-oriented tasks using the detected affordances. This framework is more extensively tested and extended to exploit detected object-action pairs for goal-oriented tasks. It adds a separate object detection pipeline applicable to a richer set of object categories than exist for existing affordance datasets. As shown in Fig. 2, the object category-agnostic affordance detector coordinates a (separately) pretrained object detector for flexible object selection during visual processing. In practice some tasks may involve multiple sub-goals, where visual information fails to seed the symbolic world state due to

occlusion; keeping track of status of objects in a scene is required. We add state memory from previous manipulation actions and their terminal states to preserve knowledge of the world state even if an action resulted in occlusions (and therefore in detection failures for the occluded objects). The overall framework translates affordances to planned action primitives for achieving multiple goal states in any order.

Contribution. This work is grounded on the premise that endowing an agent with affordance knowledge about its local environment from visual sensors provides potential action opportunities using nearby objects, which then contributes to hypothesizing action plans to achieve a goal. For robot agents to identify affordances and recognize potential interactions in an object diverse open-world, they need to understand affordances as functional properties that abstract beyond a specific set of objects, but that are shared by many objects with the similar form. As a step in this direction, this manuscript describes the *AffContext* deep network with the object category-agnostic affordance segmentation. It closes the performance gap between object-aware and object-agnostic affordance segmentation approaches. *AffContext* predicts object-action pairs to infer action opportunities on each object part across unseen categories. The obtained affordance knowledge converted into symbolic state information supports symbolic reasoning and planning with action primitives using affordance-based predicate specifications. Specifically, a system for goal-oriented task execution is presented to generate manipulation sequences by translating affordances to action primitives given a goal. Several robotic manipulation experiments ranging from simple movements, to task-oriented grasping, to goal-oriented tasks demonstrate that the approach translates to actual manipulation for an embodied robotic arm. Performance of *AffContext* is close to that of a state-of-the-art object-aware affordance recognition approach but also applies to unseen objects with the same performance. The success rate is around 96% for affordance recognition and passive exploitation (e.g., *grasp*, *contain*, *support*), and the task completion rate is 88% for active affordance exploitation using objects as tools (e.g., *cut*, *pound*, *scoop*). The results demonstrate that endowing a robot agent with affordance recognition capabilities provides it with a means to convert the recognized affordances (and objects) into executable action primitives based on simple specifications.

Related Work

Due to its primacy and role in robotic manipulation, the most commonly studied affordance has been the *grasp* affordance (Shimoga 1996; Bicchi and Kumar 2000; Bohg et al. 2014). Machine learning is increasingly being used for grasping based on the ability to learn to grasp objects (Saxena et al. 2008) for which generative or model-based methods would be difficult. Recent literature in this vein includes using a cascaded network (Lenz et al. 2015) to encode grasp features, and using deep networks to learn graspable areas (Ngiam et al. 2011) and graspable regions (Redmon and Angelova 2015; Guo et al. 2017; Chu et al. 2018). Alternatively, mapping from vision input to manipulation actions can be learned through a large collection of physical demonstrations or interactions, with Levine et al. (2016) initially taking

a supervised approach later extended to reinforcement learning (Kalashnikov et al. 2018). Robotics research on general affordances, beyond grasping, studies the potential interactions of robots with their surrounding objects and/or environments (Ugur and Piater 2015; Dehban et al. 2016; Nguyen et al. 2016b). Detecting the affordances of object parts in images is cast as a pixel-wise labelling problem and exploits computer vision approaches to segmentation. Object parts sharing the same functionality are grouped with the corresponding ground truth affordance label. Detecting affordance involves identifying applicable actions on object parts and segmenting the parts.

Affordance Recognition. Geometric cues with manually designed features were utilized for pixel-wise affordance prediction in Myers et al. (2015). The need for feature engineering was shifted to affordance-specific feature learning using an encoder-decoder convolutional neural network (CNN) architecture (Nguyen et al. 2016a). Later, the image-based approach was extended to a two-stage method (Nguyen et al. 2017) where regional features were obtained by applying object detection for object proposals on an image. Assisted by object detection, the network predicted object affordance on selected proposals from an entire input image. Building on He et al. (2017), the two-stage method was then improved by jointly optimizing object detection and affordance segmentation end-to-end (Do et al. 2018). The object category priors from the object detection branch enhance the pixel-level affordance estimates. Despite the state-of-the-art performance, annotation for detection and segmentation are labor-intensive. To reduce annotation demands in supervised learning, weakly supervised approaches instead relied on sparse key point annotations (Sawatzky et al. 2017; Sawatzky and Gall 2017). To fully avoid the requirement of costly annotation process, unsupervised learning on self-generated synthetic data was applied followed by domain adaptation techniques (Chu et al. 2019b). Since our work focuses on zero-order affordance (Aldoma et al. 2012) where affordances are functionalities found on objects and are irrespective of current states in the world, self-supervised approaches (Florence et al. 2018; Zeng et al. 2018a) lie outside of the scope of the investigation.

Optimizing detection and segmentation boosts performance through the availability of object and location priors (Do et al. 2018) but limits the transfer of learned affordance labels to unseen categories. To decouple the object category prior from the instance feature space, one solution is to detect *objectness* of a region proposal instead of predicting the object class (Chu et al. 2019a), thereby enabling category-agnostic affordance segmentation on (object) instance features. Isolating object priors from regional features permits inter-object category prediction. However, the loss of object label priors or constraints on processing requires alternative mechanisms to induce region-driven learning or spatial aggregation.

Attention and Auxiliary Tasks in Deep Networks. One means to induce contextual aggregation is to rely on object attributes. Attributes, as human describable properties, are known to assist vision tasks, such as face detection (Kumar et al. 2009, 2011), object classification (Kumar et al.

2011; Duan et al. 2012), activity recognition (Cheng et al. 2013), and fashion prediction (Liu et al. 2016). Affordances should also serve as shareable features with semantic meaning whose use could benefit feature learning for object instances. Attribute categories replace the discarded object categories during training to guide feature learning, with the aim of improving generalizability across novel object categories with recognized affordances. We extend Chu et al. (2019a) by employing attribute prediction to guide instance feature learning while removing object category supervision. The attributes include affordance as a semantic label and additional self-annotated visual attributes.

Recent studies on semantic segmentation enhance contextual aggregation by *atrous* spatial pyramid pooling and dilated convolutions (Chen et al. 2018, 2017), merging information at various scales (Zhao et al. 2017), and fusing semantic features between levels (Ding et al. 2018). To model long-range pixel or channel dependencies in a feature map, attention modules (Vaswani et al. 2017) are applied in semantic segmentation for learning global dependencies (Yuan and Wang 2018; Zhang et al. 2018; Fu et al. 2019). Region-based contextual aggregation in semantic segmentation or object-based affordance segmentation remains unexplored. Following prior works (Yuan and Wang 2018; Fu et al. 2019), we propose to incorporate a self-attention mechanism to model long-range intra-regional dependencies. The proposed architecture adopts an attention mechanism in the affordance branch and operates on object-based feature maps. Decision dependencies draw from local regions instead of the whole image. The intent behind the architecture is to guide the instance features with attribute learning, and model the dependencies within the instance feature map for affordance prediction. The improved affordance knowledge serves to aid real-world robotic manipulations.

Symbolic Reasoning for Robotics. This subsection provides a overview of task-level symbolic reasoning in robotics, with reasoning for manipulation provided in the next subsection. Once scene elements have been recognized, conversion of the information to support task or planning objectives is essential for robot agents to achieve specified goals. Establishing how to achieve the goal state from the known world state involves symbolic reasoning based methods that identify atomic actions to take in order to meet the goal specification (Ghallab et al. 2004). Symbolic planning requires planning-domain languages such as STRIPS (Fikes and Nilsson 1971), ADL (Pednault 1994), PDDL (McDermott et al. 1998), or HAL (Marthi et al. 2007). Task-level planning with symbolic reasoning through atomic actions decouples the steps from their continuous time implementation, which can fail to address barriers to execution. Combining symbolic planning with motion planning (Erdem et al. 2011; Srivastava et al. 2014) or through a hierarchical structure bridging the high-level specification and the low-level actions (Kaelbling and Lozano-Pérez 2011; de Silva et al. 2013) addresses the potential feasibility gap when considering discrete actions only. Geometric planning information establishes when pre- or post-action conditions can truly be met based on known scene structure. The motion planner may incorporate physics engines to understand

potential dynamic interactions between the robot and objects in the world and how they may open blocked paths (Stilman and Kuffner 2005; Levihn and Stilman 2014; Akbari and Rosell 2015). Likewise, differential or dynamic constraints on robot movement may need to be integrated into the motion planning module (de Silva et al. 2013; Cambon et al. 2004; Plaku and Hager 2010). Ultimately, conversion of sensor data and the goal state to a fully specified planning objective requires explicit knowledge of the object and action content of the world. To be sufficiently general, this knowledge is usually encoded within a compatible data structure whose contents are derived from an ontology (Tenorth and Beetz 2009; Chen et al. 2013). What is needed is a mechanism to connect visually sensor data to the corresponding elements in the ontology and their associated action opportunities. It often relies on visual recognition algorithms paired to items in the ontology (Tenorth and Beetz 2009; Chen et al. 2013; Pandey et al. 2012; Gravot et al. 2006) or recognition with pairwise geometric associations (Zeng et al. 2018b).

This work focuses on the perception to specification component. Low-level motion planning is simplified through action primitives with scripted plans, whose boundary conditions are determined from visual information. Object layout will be sufficiently sparse that motion planning terminal conditions are always met and motion planning can be presumed to succeed. We tackle simple, task-level reasoning for manipulation based on symbolic object and action knowledge extracted from visual recognition algorithms.

Symbolic Reasoning for Manipulation. With regards to scene understanding, robotic manipulation research that focuses on the ontology and the underlying reasoning framework employs (or assumes the existence of) tagged objects or recognition algorithms tuned to the objects used (Tenorth and Beetz 2009; Chen et al. 2013; Pandey et al. 2012; Zeng et al. 2018b). The setup simplifies the perception problem. A less relaxed scene simplification is to have it consist of planar objects, boxlike objects, or uniquely colored objects (Ugur and Piater 2015; Gaschler et al. 2015; Migimatsu and Bohg 2020; Suárez-Hernández et al. 2018; Winkler et al. 2012). Alternatively, it may rely on simulation (Stilman and Kuffner 2005; Akbari and Rosell 2016; Gravot et al. 2006; Suárez-Hernández et al. 2018) since object properties in simulation are precisely known and action execution can be guaranteed (through reduced fidelity to real-world dynamics). These implementations create an experiment to reality gap in the robotic system that prevents more general use of the underlying ontological framework or manipulation strategies. However, they also permit deeper investigation into joint symbolic and motion planning strategies that incorporate more advanced elements, such as probabilistic planning, optimality, linguistic imprecision, and action execution failure detection (Toussaint et al. 2010; Winkler et al. 2012).

With regards to the action specifications, this symbolic knowledge can be formed by interactive experiences with the environment through manipulation exploration (Ugur and Piater 2015). Achieving the same outcomes without relying on simple, coded scenarios in order to work for more realistic and less constrained visual content requires

connecting to advances in computer vision (Yang et al. 2015). However, there is a tension between inferring models from annotated data or experience versus using pre-specified models (Chen et al. 2013). Following Chen et al. (2013), we first aim to use a pre-specified model in this paper before considering the augmentation of the action specifications through demonstration or additional learning (which will be left to a future investigation). Emphasis will be on using known affordance categories, as perceived from visual sensors, to seed symbolic planning specifications for manipulation.

On the perception to specification front, manipulation with symbolic reasoning involving visual processing mainly deals with object poses and inter-object spatial relationships (Sui et al. 2017; Zeng et al. 2018b). Task specifications involve rearranging a scene to match a given target arrangement. Doing so requires estimating scene graphs for the 6D poses and inter-object relations of objects from RGB-D input imagery (Liu et al. 2020). The scene graph describes object configurations using a tree structure, which can then translate to specifications for goal-directed robot manipulation plans in low clutter settings (Sui et al. 2017; Zeng et al. 2018b). Both the initial and goal states are given as RGB-D images to be converted into estimated poses and relations described within the axiomatic scene graph, whose transcription to PDDL supports symbolic planning. Other forms of symbolic knowledge besides spatial properties can also be used to define manipulation planning objectives, with affordances and their intra-object interactions being one important class of symbolic knowledge. Affordances can support general purpose vision-based manipulation planning by providing awareness of potentially executable atomic actions for a given scene. Using predefined object-task affordances, high-level symbolic knowledge is shown to improve prediction of grasping location for specific tasks with low-level visual shape features (Antanas et al. 2019), which tackles the linkage between symbolic planning and geometric planning. Scene understanding involving affordance recognition on realistic objects is less explored.

Commonly seen affordances are considered in Antanas et al. (2019). However, the affordances are predefined instead of predicted from visual context. We aim to bridge the research gap of predicting affordance information from visual input to support reasoning via symbolic planning for solving goal-oriented manipulation tasks. Specifically, we consider predicates modeled from object part functionality (and object states) as opposed to object spatial relations. The available action states are inferred from the scene through affordance estimates (and object recognition in some cases). We show that visual input can be converted into symbolic knowledge for use by a PDDL planning solver to generate a sequence of executable atomic actions whose execution achieves the desired goal state.

Approach

There are two main objectives that aim to be linked to achieve specification-based manipulation supported by affordance reasoning. Given a corresponding pair of color and depth images, the first objective is to identify pixel-wise affordances of object parts for seen and unseen object

categories. The second objective is to connect the affordance reasoning module with a symbolic planning system so that the recognized affordances can seed the initial state of the symbolic planner. The provision of a specified goal state would then generate a sequence of manipulation actions that change the initial state of the world to meet the goal state. This section covers the design of the affordance recognition CNN and its merger with a PDDL planner.

Basic CNN Design

The general structure of the deep network design for jointly predicting object regions and their affordance segmentations across novel categories is depicted in Fig. 3. The network, called *AffContext*, adopts a two-stage architecture (He et al. 2017; Do et al. 2018) with VGG-16 (Simonyan and Zisserman 2015) as a backbone. It builds on earlier work (Chu et al. 2019a) with a similar pipeline, but includes modifications intended to improve affordance segmentation. The first stage generates region proposals whose feature descriptors are then input to separate detection and segmentation branches for predicting object regions and affordance maps, respectively. More specifically, the shared feature map ($38 \times 63 \times 512$ feature) from the intermediate convolutional layers (layer 13 of VGG-16) are sent to the *Region Proposal network* for region proposals; the two ROI align layers (He et al. 2017) feed the collected instances to the task branches. After the first stage, two processing branches follow. To support generalized learning for the segmentation branch (bottom) to novel categories, the detection branch (top) performs binary classification to separate foreground objects from the background. The segmentation branch takes in category-agnostic object regions for predicting the affordance map within each region. To address the contextual dependencies and the non-local feature learning within a region proposal, we introduce two improvements, attention and attributes, described next. They enhance the associations among local features and guide feature learning to be object aware but not object specific.

Region-based Self-Attention

The goal of object part affordance segmentation is to group pixels sharing the same functionality and to assign them the correct affordance labels. In urban street semantic segmentation (Cordts et al. 2016; Richter et al. 2016), the entire scene usually corresponds to large subset of possible ground truth labels. In contrast, affordance segmentation assigns labels to object regions only, with the assigned labels being a small subset relative to the set of known affordance labels. The semantic context of the image region (e.g., a cup) narrows the set of relevant affordances (e.g., grasp, contain) and thus reduces the search space (Zhang et al. 2018). Since object category semantic priors require object-specific detection modules that are not part of the network design, alternative means to inform the segmentation are necessary. Given that form and function are often correlated, the missing object prior information could be recovered by having the pixel-wise decisions depend on non-local pixel features that may already encode for visual structure (form) related to affordances (function). Doing so compensates for

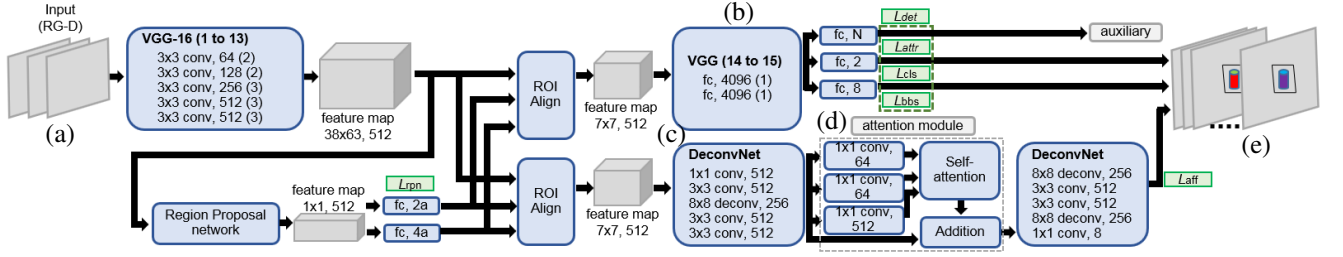


Figure 3. Network structure of the proposed detector with self-attention and attribute learning. The network predicts affordances of object parts for each object in the view. Blue blocks indicate network layers and gray blocks indicate images and feature maps. (a) RG-D images are input of the network; (b) Category-agnostic proposals with *objectness* are forced to predict attributes during training as an auxiliary task; (c) Deconvolutional layers lead to a fine-grained feature map for learning long-range dependencies; (d) Self-attention mechanism operation is incorporated in affordance branch on the intermediate feature ($30 \times 30 \times 512$); (e) The final output includes bounding boxes and multiple layers indicating confidences for affordances on a single pixel.

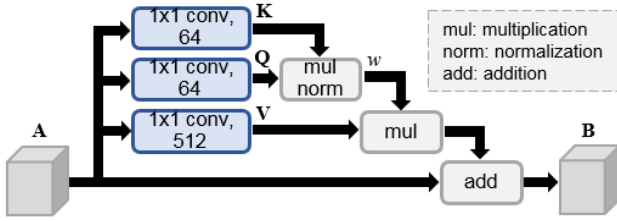


Figure 4. Details of the attention module for regional features in affordance branch. \mathbf{K} , \mathbf{Q} and \mathbf{V} refer to key, query and value, respectively

the small receptive field of convolutional operations and provides more global context for local pixel-wise decisions.

To incorporate non-local contextual information, the network architecture and learning process explicitly creates associations between local features of pixels within a region proposal. A self-attention mechanism, as depicted in Fig. 4, on the segmentation branch adapts long-range contextual information. Given an instance feature map $\mathbf{A} \in \mathbb{R}^{c \times u \times v}$, a triplet of *key* $\mathbf{K} \in \mathbb{R}^{c \times u \times v}$, *query* $\mathbf{Q} \in \mathbb{R}^{c \times u \times v}$ and *value* $\mathbf{V} \in \mathbb{R}^{c \times u \times v}$ feature maps are predicted. The contextual relationship w_{ji} uses a spatial attention module for features at pixel positions j and i within the instance feature map:

$$w_{ji} = \frac{1}{Z_j} \exp(Q_i^\top K_j), \quad (1)$$

where w_{ji} indicates the degree that the i^{th} representation feature influences the j^{th} feature. Z_j is the normalization term:

$$Z_j = \sum_{i=1}^{u \times v} \exp(Q_i^\top K_j). \quad (2)$$

To aggregate the predicted correlation between features in different positions within a region proposal, the feature map \mathbf{V} is associated with contextual relationship w_{ji} and learns a residual function with the original feature map \mathbf{A} to provide the final output $\mathbf{B} \in \mathbb{R}^{c \times u \times v}$. For features at pixel position j :

$$\mathbf{B}_j = \alpha \sum_{i=1}^{u \times v} (w_{ji} \mathbf{V}_i) + \mathbf{A}_j \quad (3)$$

where α is a learnt scale parameter that influences the weighting between the original feature vector \mathbf{A}_j and the attentional feature vector.

Affordance as Auxiliary Task and Attribute

Having an object detection branch with binary classification removes contextual information provided by the object category. While it does provide category-agnostic processing, it does not leverage potential information that may be transferable to unseen object instances. Thus, in addition to predicting *objectness* through object detection, the detection pathway is augmented with a multi-class classification module. The module works as an auxiliary task to explicitly predict existing affordances in a candidate region. The network is trained to predict existing affordances across categories, which transfer to unseen categories during deployment. Predicting affordances at the pixel-level and at the region level are related processes. Though a segmentation model may internally learn to predict possible affordances within a region, explicitly guiding the learning process using an auxiliary task may allow two tasks to positively influence each other (Jaderberg et al. 2017; Li 2017; Zhang et al. 2015).

Since affordance labels apply to objects outside of the training set, predicting existing affordances for a region proposal can be treated as predicting shareable attributes across object categories. Attribute learning enhances object classification when suitable attributes are available (Farhadi et al. 2009; Li et al. 2010; Sun et al. 2013). In the auxiliary module, affordances are directly treated as attributes to enhance the learning of visual representation. Based on the potentially similar visual properties of objects with similar functions, affordances may be recognizable attributes of unseen objects based on their visual appearance. If this relationship can be captured by incorporating attribute estimation into the detection branch, then it will enhance learning visual representations related to affordance.

For clarity, below we refer to affordances from the auxiliary module as *attributes* (or *affordance attributes* in long form), and reserve the simple term *affordance* for the pixel-wise segmentation case. To guide the feature learning of each region proposal, a sub-branch parallel to *objectness* detection and bounding box regression is augmented to perform attribute prediction with N outputs, where N is the number of affordance attributes defined across categories. Each attribute output is a binary classification predicting whether a specific attribute (affordance) is found in the region proposal, based on the instance feature shared with *objectness* detection and bounding box regression.

The *objectness* branch identifies foreground from background and hence the class number is $C = 2$. Let $\rho \in \mathbb{R}^1$ denote the probability of an instance being foreground, $\beta \in \mathbb{R}^4$ denote the corresponding bounding box, and $\alpha \in \mathbb{R}^N$ denote the corresponding probabilities of attributes within the instance region. Define the loss function of the complete detection branch (\mathcal{L}_{det}) to be:

$$\mathcal{L}_{\text{det}}(\{(\rho, \beta, \alpha)\}_{c=0}^{C-1}) = \sum_c \mathcal{L}_{\text{cls}}(\rho) + \lambda_1 \sum_c \delta_{c,1} \mathcal{L}_{\text{bb}}(\beta_c, \beta_c^*) + \frac{\lambda_2}{N} \sum_c \delta_{c,1} \sum_i^N \mathcal{L}_{\text{att}}(\alpha_i). \quad (4)$$

where \mathcal{L}_{cls} denotes the cross entropy loss for *objectness* classification (cls), \mathcal{L}_{bb} denotes the l_1 loss for bounding box (bb) regression with β_c^* the ground truth annotation, and \mathcal{L}_{att} denotes the binary cross entropy loss for each attribute. The scalars λ_1 and λ_2 are optimization weight factors, and $\delta_{\cdot, \cdot}$ is the Kronecker delta function.

Regional Attention and Attribute Embedding

The regional attention and attribute learning modules are added to the final network. The attribute learning parallel to the foreground detection works as an auxiliary task to guide feature learning during training; it is discarded during inference. The attention module in the segmentation branch learns a representation of a region proposal that gathers contextual information; it is applied during inference. To have a higher resolution affordance mask and to learn long-range dependencies, deconvolutional layers initially upsample the feature map of the segmentation branch (bottom in Fig. 3). Attention is applied after the first deconvolutional operation on the 30×30 feature map, followed by two deconvolutional operations for the final 244×244 affordance map. To compute the loss for the affordance, let $q(j, a)$ denote the predicted affordance mask on a RoI-based feature map, where $j \in \text{RoI}$ is the j^{th} pixel in a region proposal, and $a \in A$ is the a^{th} affordance at the pixel. The affordance loss \mathcal{L}_{aff} is defined as multinomial cross entropy loss:

$$\mathcal{L}_{\text{aff}} = - \sum_{j \in \text{RoI}} \frac{1}{|\text{RoI}|} \sum_{a \in A} Y(j, a) \log(q(j, a)) \quad (5)$$

where $|\text{RoI}|$ is the total area of the region of interest, Y is the ground truth of the corresponding affordance mask with A channels.

The overall network inherits Faster-RCNN (Ren et al. 2015) on a VGG16 (Simonyan and Zisserman 2015) backbone with modified detection and segmentation branches while keeping the region proposal network (RPN) intact. Let \mathcal{L}_{rpn} denote the RPN loss from the original network, the loss for the entire network is:

$$\mathcal{L}_{\text{tot}} = \mathcal{L}_{\text{det}} + \mathcal{L}_{\text{rpn}} + \mathcal{L}_{\text{aff}}. \quad (6)$$

Planning with PDDL

Goal-oriented manipulation may require an agent to achieve a goal state via a sequence of atomic actions, with each action involving an intermediate state change of the objects

in the environment and/or the manipulator. As a standard and widely used planning language, Planning Domain Definition Language (PDDL) is adopted to encode and generate the desired sequence of actions. The PDDL takes a **domain** definition and a **problem** description. The **domain** pre-defines a list of **predicates** and corresponding effects, while the **problem** includes the initial state and goal state descriptions. To utilize the PDDL, the initial state required by the PDDL algorithm is acquired via predictions for objectness and the predicted objects' corresponding affordances in the image. Together with the goal state, the planned sequence is solved by Fast Downward (Helmert 2006) as a list of executable atomic actions for a robotic manipulator.

To handle scenarios where determining an object category is required, incorporating a general pre-trained object detector enables selecting from multiple tools with similar functionality in the view, improving the flexibility of use cases. To further handle scenarios where an intermediate goal exists, a *state keeper* is added to the PDDL to preserve the terminal state from the previous planning session. Such a mechanism is essential since both detectors (*objectness* and the additional *object-specific*) tend to miss an object when it is inside of another object. Persistence of planned state information aids multi-step or sequential planning as depicted in Fig. 2, where the sequentially applied goal states benefit from state persistence. Incorporating *object detector* and *state keeper* with the PDDL allows goal-oriented manipulation with tool selections, as well as reusing states for consecutive goals. Goals such as “*place an object into a specific container and then place the second object into any empty container*” become possible.

Vision Evaluation

This section describes the training process and benchmarking results of the affordance prediction network *AffContext*. Relative to the complete perceive, plan, act processing pipeline of a complete implementation on a robotic arm, it focuses on the perception component and tests performance as a visual processing algorithm absent the embodied manipulation components. The training dataset is described, as well as the training method, followed by the baseline approaches and benchmarking results.

UMD Dataset

The UMD dataset (Myers et al. 2015) covers 17 object categories with 7 affordances. The objects are from kitchen, workshop, and garden settings. The dataset contains 28k+ RGB-D images captured by a Kinect sensor with the object on a rotating table for data collection. The annotated segmentations provide affordance label ground truth for each object part. The additional ground truth of object bounding boxes is obtained by filtering out the background table from the foreground objects, and establishing a tight rectangular bounding box. The UMD dataset has *image split* and *category split* benchmarking approaches. Evaluation uses the *category split* benchmark, which tests unseen categories.

Data Preprocessing and Training

The proposed approach reuses the weights of VGG-16 (Simonyan and Zisserman 2015) pre-trained on ImageNet

Table 1. Images per Affordance

affordance	images	affordance	images	affordance	images
grasp	18235	contain	7889	wrap	5250
cut	5542	pound	2257		
scoop	2869	support	2317		

(Deng et al. 2009) for initialization. The layers for attribute prediction and for the affordance branch, including the attention module, are trained from scratch. To incorporate RGB-D images for geometric information with pre-trained weights, the blue channel is substituted with the depth channel (Redmon and Angelova 2015; Chu et al. 2018). Ideally, any channel can be replaced with the depth channel. The value of depth channel is normalized to the range $[0, 255]$ with 144 as the mean value. Missing value or *NaN* in depth channel is filled with 0. The whole network is trained end-to-end for 5 epochs. The training starts with initial learning rate $r = 0.001$ which is divided by 10 for every 2 epochs. Training time is around 3 days with a single Nvidia GTX 1080 Ti.

Baseline Methods

In addition to including published outcomes for the UMD Benchmarking Dataset, several sensible approaches serve as baselines. They arise from partial or alternative implementation of *AffContext* algorithm, based on the earlier work (Chu et al. 2019a). The first *baseline* approach, labelled *Obj-wise*, is a deep network structure trained with *objectness* detection only, i.e., without regional attention, and without attribute embedding. It is a modified version of *AffNet* (Do et al. 2018) with object category labels unused during training on the *category-split* data. The network only outputs the primary affordance. A second *baseline* approach, denoted *KLdiv* (Chu et al. 2019a), uses the *Obj-wise* network and replaces the cross-entropy loss, \mathcal{L}_{aff} , with KL-divergence for ranked affordance outputs. Specifically, since each object part is assigned from one to three ranked affordances by human annotators, *KLdiv* treats the ranking of affordances as a distribution and learns to predict ranking during inference time. The ranking output permits secondary affordance of an object part. A third *baseline*, denoted *Multi*, also employs the *Obj-wise* network. To permit prediction of multiple affordances on the same object part, *Multi* simply replicates the segmentation branch to provide a segmentation for affordance (e.g., one-vs-all). The *Multi* segmentation branch grows in direct proportion to the affordance rank quantity (here three). It is a straightforward, brute force method used for comparison (Chu et al. 2019a). Another *baseline* for segmentation employs a modified DeepLab (Chen et al. 2018; Chu et al. 2019a). DeepLab is a widely adopted segmentation network for semantic segmentation, especially for urban street segmentation (Ros et al. 2016; Richter et al. 2016). It is a representative image-based segmentation approach for comparison. With regards to *AffContext*, the implementation is also modified to permit ranked affordances by using the KL-divergence instead of the cross-entropy loss. However, due to the neural network’s memory footprint, only the regional attention mechanism is incorporated (no attribute embedding). We label it *AffContext_{KL-att}*.

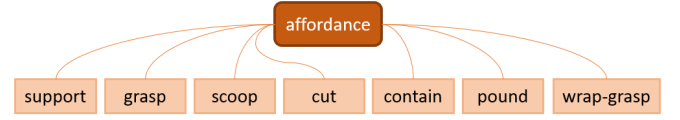


Figure 5. Affordances are used as attributes in an auxiliary module for per-candidate region multi-class classification in the UMD dataset.

For the auxiliary task used during *AffContext* training, we treat the original UMD affordance labels as attributes across categories, see Fig. 5. In total seven attributes (number of affordance) are defined for representing the UMD tool dataset, as summarized in Table 1.

Evaluation Metric

To evaluate the affordance segmentation responses, derived from probability outputs over affordance classes, against ground truth labels for each affordance, we adopt the weighted F-measures metric, F_{β}^{ω} , for the predicted masks:

$$F_{\beta}^{\omega} = (1 + \beta^2) \frac{Pr^{\omega} \cdot Rc^{\omega}}{\beta^2 \cdot Pr^{\omega} + Rc^{\omega}}. \quad (7)$$

where Pr^{ω} and Rc^{ω} are the weighed precision and recall values, respectively (Margolin et al. 2014). Higher weights are assigned to pixels closer to foreground ground truth. The weighted F-measures outputs lie in the range $[0, 1]$. A second metric evaluates the prediction performance of the rankings for multiple affordance on object parts and applies to the KL-divergence trained network. It is the *ranked* weighted F-measures metric, F_{β}^{ω} ,

$$R_{\beta}^{\omega} = \sum_r \omega_r F_{\beta}^{\omega}(r), \quad \text{with} \quad \sum_r \omega_r = 1, \quad (8)$$

where ω_r are the ranked weights contributing to the weighted sum over the corresponding affordances (Margolin et al. 2014). The top affordance receives the most weight and so on, per $\omega_r = 2^{-r} / \sum_{r'} 2^{-r'}$. The ranked weighted F-measures outputs lie in the range $[0, 1]$.

Evaluation results are obtained by running the same evaluation code provided by UMD (Myers et al. 2015). All the parameters are the same. There are two parameters associated with ω including σ and α . Specifically, $\beta = 1$, $\sigma = 5$, and $\alpha = \frac{\ln 0.5}{5}$.

Benchmarking on UMD Novel Objects

The traditional benchmarking scheme for the UMD dataset is to perform an image-split test, where all object categories are represented. Affordance evaluation is performed only for the known object categories. Top performance for the image-split test lies in the range of 0.733 to 0.799 for the weighted F-measures (Nguyen et al. 2016a; Do et al. 2018; Chen et al. 2018). The category-split test, where some object categories are excluded is a more difficult problem since top performing methods rely on the object category prediction to provide a prior on the potential affordances. The weighted F-measures decrease for the category-split test and there are less reported evaluations. Especially when considering evaluation for weighted F-measures and ranked weighted F-measures. For

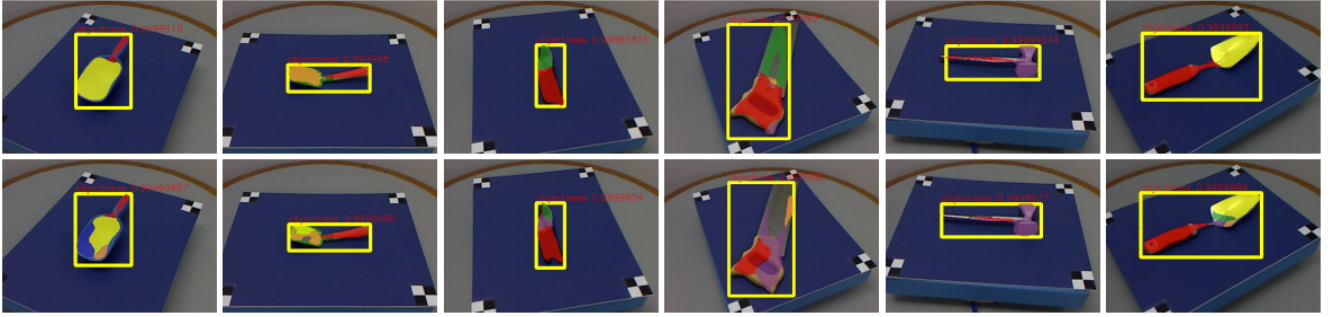


Figure 6. Affordance segmentation results on UMD benchmark, where color overlays represent affordance labels, red: grasp; yellow: scoop; green:cut; dark blue: contain; blue: wrap-grasp; orange: support; purple: pound. **Top:** results using *AffContext*; **Bottom:** results using *Obj-wise* baseline.

Table 2. Affordance Segmentation Performance On UMD Dataset (novel category).

	weighted F-measures							
	grasp	cut	scoop	contain	pound	support	w-grasp	average
Rezapour Lakani et al. (2019)	0.46	0.30	0.22	0.47	0.08	0.03	0.47	0.29
DeepLab (Chu et al. 2019a)	0.55	0.30	0.36	0.58	0.42	0.22	0.93	0.48
Obj-wise (Chu et al. 2019a)	0.61	0.37	0.60	0.61	0.81	0.59	0.94	0.64
KLdiv-1 (Chu et al. 2019a)	0.54	0.31	0.39	0.63	0.55	0.75	0.92	0.58
Multi-1 (Chu et al. 2019a)	0.56	0.35	0.53	0.60	0.69	0.68	0.92	0.62
<i>AffContext</i>	0.60	0.37	0.60	0.61	0.80	0.88	0.94	0.69
<i>AffContext</i> _{KL-att-1}	0.54	0.37	0.42	0.62	0.63	0.87	0.92	0.63

Table 3. Affordance Ranking Performance On UMD Dataset (novel category)

	ranked weighted F-measures							
	grasp	cut	scoop	contain	pound	support	w-grasp	average
HMP (Myers et al. 2015)	0.16	0.02	0.15	0.18	0.02	0.05	0.10	0.10
SRF (Myers et al. 2015)	0.05	0.01	0.04	0.07	0.02	0.01	0.07	0.04
VGG (Sawatzky et al. 2017)	0.18	0.05	0.18	0.20	0.03	0.07	0.11	0.12
ResNet (Sawatzky et al. 2017)	0.16	0.05	0.18	0.19	0.02	0.06	0.11	0.11
Rezapour Lakani et al. (2019)	0.19	0.18	0.28	0.32	0.08	0.11	0.32	0.21
DeepLab (Chu et al. 2019a)	0.299	0.172	0.101	0.223	0.056	0.037	0.531	0.203
KLdiv (Chu et al. 2019a)	0.322	0.175	0.178	0.232	0.093	0.096	0.525	0.232
Multi (Chu et al. 2019a)	0.336	0.200	0.211	0.247	0.082	0.109	0.526	0.244
<i>AffContext</i> _{KL-att}	0.331	0.184	0.183	0.254	0.101	0.103	0.533	0.241

example, DeepLab performance drops by 34.5% (to 0.48 from 0.733). Since this study aims to explore affordance recognition in the absence of object category knowledge, the category-split test case is performed for single affordance and ranked affordance prediction. Published baselines are included in the benchmarking results when available. When presenting the results, the table contents will be organized according to (i) published results, (ii) strong baselines created in earlier efforts (Chu et al. 2019a), and (iii) the current results for *AffContext*.

Novel Category Affordance Prediction. Qualitative results of *AffContext* are depicted in the top row Fig. 6, which has color overlays of the affordance predictions on the objects. The bottom row shows the same for the best performing baseline approach per Table 2, which is the *Obj-wise* implementation. *AffContext* improves the consistency of affordance segmentation as seen by less oversegmentation and more spatially uniform affordance labels.

Quantitative evaluation using the weighted F-measure for the UMD benchmark is found in Table 2, with available published outcomes for the category-split test. For the multi-affordance *KLdiv* baseline, the top ranked affordance is

taken as the affordance output. Hence the label *KLdiv-1*. Likewise the single affordance version of *AffContext*_{KL-att} outputs only the top ranked affordance label (denoted *AffContext*_{KL-att-1}). *AffContext* has the strongest performance, with the *Obj-wise* baseline next. Compared to the best published result, the proposed approach achieves a 43% improvement (0.48 to 0.69). Compared to the strong baseline, it achieves 7% improvement over *Obj-wise*. Meanwhile *AffContext*_{KL-att-1} has a 1.5% drop in performance relative to *Obj-wise*, while the non-attention version *KLdiv-1* has a 9.4% drop in performance. The attribute and attention modules lead to improved performance in the primary affordance segmentation outcomes.

Novel Category Affordance Ranking. Affordance ranking with ranked weighted F-measures is reported in Table 3. This test is harder, due to the metric heavily penalizing incorrect rankings, which compresses the score output values. The results show that *AffContext* outperforms the existing published approaches and most strong baselines for novel object categories. Compared to the most recent published results (Rezapour Lakani et al. 2019) and to the strong baseline DeepLab, *AffContext* improves by 14%

Table 4. Ablation Study

	module		weighted F-measures							
	attent	attri	grasp	cut	scoop	contain	pound	support	w-grasp	average
Obj-wise			0.61	0.37	0.60	0.61	0.81	0.59	0.94	0.64
Obj-wise		✓	0.62	0.33	0.51	0.61	0.81	0.79	0.94	0.66
Obj-wise	✓		0.60	0.40	0.67	0.60	0.78	0.75	0.94	0.68
Obj-wise	✓	✓	0.60	0.37	0.60	0.61	0.80	0.88	0.94	0.69

and 20%, respectively. Evaluation of $AffContext_{KL-att}$ relative to $KLdiv$ and $Multi$ shows that $AffContext_{KL-att}$ outperforms $KLdiv$ and almost matches $Multi$. Recall that the implementation of $Multi$ (Chu et al. 2019a) in Table 3 is especially designed for affordance ranking by adopting multiple affordance branches for each rank output. Consequently it scales in parameter size linearly with the rank quantity (three). The $KLdiv$ approach does not impact the parameter size of the affordance ranking branch (compared to cross-entropy loss). The $AffContext_{KL-att}$ approach increases by less than 1% the branch network size. The gap between $KLdiv$ (0.2315) and $Multi$ (0.2444) is 5.3%. In contrast, for a less than 1% increase in branch parameters, $AffContext$ (0.2414) reduces the performance drop to 1.2%. In essence, for a small increase in size the attention module almost matches the performance of the brute force (one-vs-all) network. Given that $AffContext_{KL-att-1}$ outperforms $Multi$ for the primary affordance, per Table 2, the main output differences lie with the secondary and tertiary affordances.

Ablation Study

Table 4 shows the ablation study results for $AffContext$, where the baseline network is the $Obj-wise$ network (first row). The second and third rows quantify the improvements gained from regional attention and attribute learning, respectively. The last row reports the performance with both attention and attribute learning together, which achieves the best result. Each design is independently trained with ImageNet pre-trained weights, instead of finetuning one-by-one. While a 3.7% (0.770 to 0.799) improvement in Do et al. (2018) was regarded as reasonable achievement on UMD image-split benchmark, the ablation study shows 3.1% and 6.2% improvements by introducing attribute learning and ROI-based attention individually. Furthermore, the current gap between the best performing object-aware approach (0.799 for Do et al. (2018)) and the best performing object-agnostic approach (0.48 for DeepLab) has been reduced from a 40.0% drop to a 13.6% drop and lies close to the lower-end of the range for state-of-the-art object-aware methods (0.733-0.799), e.g., within 6%. The next section, which performs manipulation tests, will further explore how this difference manifests when considering task-relevant manipulation activities, from simply grasping and picking up an object, to performing affordance aware manipulation tasks.

Affordance Detection across Datasets

The last vision-only test demonstrates generalizability across datasets. $AffContext$ trained on the novel-category split of the UMD dataset is applied to the Cornell dataset (Lab 2013). The Cornell dataset consists of 885 images of 244 different objects for learning robotic grasping. Each image is labelled



Figure 7. Comparison on Cornell dataset. **Top:** detection results of $AffContext$ method. **Bottom:** $Obj-wise$ model.

with multiple ground truth grasps. Though affordance masks are not available for quantitative evaluation with F_{β}^w and ranked F_{β}^w metrics, visualizations of qualitative results and comparisons are presented in Fig. 7. Similar to Fig. 6, the outcomes here have more consistent and continuous affordance segmentations for $AffContext$ versus $Obj-wise$.

Manipulation Experiments and Methodology

Beyond vision-only benchmarking, embodied robotic manipulation with affordance detection is tested and evaluated. The physical manipulation tests use a custom-built 7-DoF robotic manipulator and a Microsoft Kinect using an eye-to-hand configuration (see Fig. 8). In the experiment setting, the sensor input includes depth information. Image areas with target affordances are mapped to 3D space for manipulation planning and execution. Multiple scenarios and possible applications are validated. This section describes the experimental methodology of the five test scenarios, with the subsequent section covering the results.

Affordance on Seen Categories

As in Do et al. (2018), commonly seen *grasp* and *contain* affordances are first examined. In addition, the *support* affordance is included. All the objects in this experiment are selected from categories in UMD dataset, and thus can be recognized by $AffNet$ (trained on UMD dataset). Two instances are picked in each category, where one is similar to instances in UMD dataset, and the other is dissimilar. Examples of selected similar and dissimilar objects are shown in Fig. 9. The experiment is mainly designed for benchmarking the proposed category-agnostic detector against the state-of-the-art affordance detection (Do et al. 2018), which is trained with object prior but limited to the training categories during deployment.

For experiments involving the *grasp* affordance, the grasp center is computed by averaging the *grasp*-able pixels, with grasping orientation determined by fitting a line to predicted pixels. Since the camera is set near top-down view,

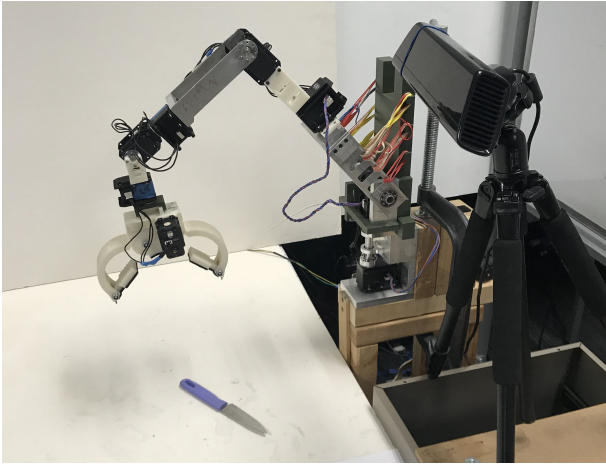


Figure 8. Experimental setup for eye-to-hand physical manipulation, with a 7 DoF manipulator and a Microsoft Kinect RGB-D sensor.

the orientation is then corrected by the relative orientation between the input sensor and working space. For the *contain* and *support* affordances, a small cuboid is placed into (or onto) an object predicted as *contain-able* (*support-able*) with the robotic arm. As with the *grasp* affordance, the location is determined by averaging the pixels predicted as *contain-able* (*support-able*). The evaluation metric is discussed in the next section.

Affordance with Multiple Objects

More common scenarios usually involve multiple objects in a scene. The workspace may contain task-irrelevant objects. For instance, the robotic arm is required to grasp a knife while a plate and cup are in the scene. The manipulator is asked to put an object into the cup while knife and spoon are around. Though the proposed method is trained on UMD dataset with single object annotated in each image, the trained model is readily available to detect multiple objects with corresponding affordance maps. This experiment replicates the first one, but uses a dissimilar set of objects, such that there are no common affordances. For each trial, multiple objects (at least 3) including the target object (with the target affordance) are presented and randomly placed in a visible and reachable area. The experiment tests affordance recognition correctness and consistency in the presence of nuisance categories. If another object is misattributed the target affordance, then the planner may output an incorrect action sequence.

Affordance on Unseen Categories

This experiment tests generalizability to unseen categories. Having this capability can mitigate labor-intensive pixel-wise and bounding box annotations. While *AffNet* achieves slightly better vision performance, it is limited to the categories existing in training set (17 object categories in UMD dataset). Therefore, when replicating the first experiment, it modifies the object set to draw from objects not seen in the UMD object categories.



Figure 9. Examples of similar (top row) and dissimilar objects (bottom row) relative to the UMD dataset. (a) and (d): Most mugs are small and have no or few visual patterns; the dissimilar mug is large and has patterns. (b) and (e): Most spoons large serving spoons; the dissimilar spoon is a small toy. (c) and (f): Most turners are made of wood or steel; the dissimilar turner is made of plastic.

Affordance for Task-Oriented Grasping

Affordances such as *grasp*, *contain* and *support* are usually considered independently from the manipulation perspective. In contrast, some affordances like *pound* and *cut* are commonly utilized in combination with *grasp* and a corresponding action primitive. Task-oriented grasping experiments were designed to evaluate these affordances. Task-oriented grasping requires identifying a proper graspable part and functional part in order to accomplish the task. In this section, two task-oriented grasping experiments including *pound peg into slot* task and *cut through string* task are described.

The *pound peg into slot* task is setup as shown in Fig. 10(a). The peg is initially inserted half-way into a slot and placed within reach of the manipulator. The manipulator is required to detect and grasp the tool, then use it to pound the peg fully into the slot (three strikes are programmed for each trial). Solving it involves using the *grasp* affordance to grab the object. The distance between the grasping point and the functional point (where to pound on the hammer head) is computed from the affordance map and depth image. The Aruco marker at the top of the box is for detecting the relative location of the peg.

The second task, *cut through string*, is shown in Fig. 10(b). The string is a twisted tissue fixed vertically between two horizontal surfaces and taped to them at each end. The manipulator is required to find and grasp the handle of the tool, and cut the string off horizontally using a programmed wrist motion (three slice motions are programmed for each trial). Again, the Aruco marker is for detecting the location of the string, while the grasping point and cutting point is computed through the affordance map and depth image.

Affordance with modified PDDL pipeline

Category-agnostic affordance detection generalizes learned affordances to unseen categories by detecting objectness instead of identifying specific object classes. However,

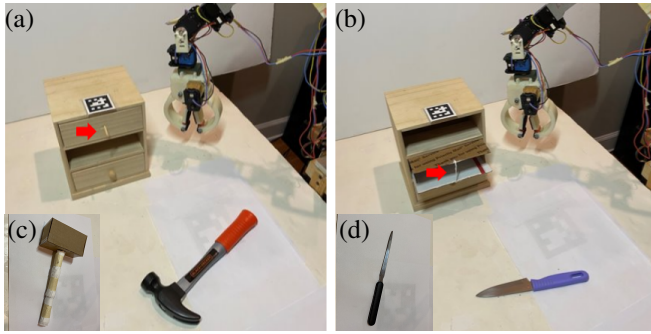


Figure 10. Illustration of task-oriented manipulation settings. **(a)** *peg into slot task*: A peg (see red arrow) is half-way through the slot. The manipulator needs to grasp the tool (hammer or tenderizer) and pound the peg fully into the slot. **(b)** *cut through string task*: A string made by tissue is attached vertically (see red arrow). The manipulator needs to grasp the tool (knife or letter opener) and fully cut off the string. **(c)** Custom-made toy tenderizer. **(d)** Letter opener.

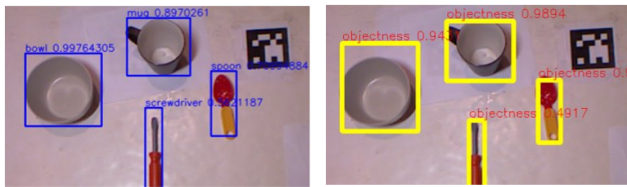


Figure 11. Left: Candidate bounding boxes (in blue) predicted by a pre-trained object detector. Right: Candidate bounding boxes (in yellow) predicted by proposed affordance detector. The detectors are independently trained yet predict candidates that are close in locations and similar in size.

knowing object classes may be required in some scenarios such as grasping a tool from a toolbox, or pouring water into a cup next to a bowl. This can be completed by using the object-agnostic affordance detector with a pre-trained (affordance-agnostic) object detector. In this experiment, an object detector (Faster-RCNN with a VGG-16 backbone) is trained on 21 objects (items commonly seen at home or on office table). As shown in Fig. 11, though the affordance and object detectors are trained independently, they both predict similar candidate bounding boxes in our setting. The predictions from the two detectors are associated through overlapping bounding box locations and similar sizes. To increase the complexity of the task, this experiment looks at compound task specifications where the objects have coupled or interacting specifications. It also involves scene states that have objects on or in other objects, which result in reduced detection and recognition probability. Missed detections or recognitions mean the state cannot be established from the recovered visual information. Keeping track of the symbolic state and its spatial parameters via the *state keeper* is necessary. These tasks require the *state keeper* module to transfer the terminal state of the prior action to the initial state of the subsequent action. An example would be the state *plate contains spoon* as well as the location of the spoon in scene. Four experiments are designed to evaluate the full pipeline, which includes the *pre-trained object detector* and the *state keeper*.

The first two experiments, *pick knife/spoon into bowl* and *select trowel/spoon to scoop beans* examine the combined use of object detection and affordance recognition to

select from objects in the view to accomplish the tasks. Additionally, it is designed to have a nuisance object in the scene with similar affordances. Consider the first experiment. Though both objects are in the scene, at the commencement of each trial the *knife* or *spoon* is randomly selected to be the object to place into the bowl so that the other becomes the nuisance object. The object detector is required to identify the chosen object, while the affordance recognition process is needed to *grasp* it. Likewise, the pipeline should correctly interpret the bowl in the scene. It implicitly tests the ability of the two detectors to identify the same object regions, as in Fig. 11, and to recognize their object types and affordances. The equivalent setup and objective applies to the second experiment, *select trowel/spoon to scoop beans*.

For some deployments, the robot manipulator may not get a single task to perform, but may get a series of tasks spaced out in time, that may or may not be related. Awareness of prior activities is important when the resulting states impede visual processing or scene reasoning. It is a form of scene graph reasoning, but based on executed tasks and exploited object affordances. The last two experiments, *put spoon on plate then move to bowl* and *place objects into empty containers* further require the *state keeper* to keep track of the state of the scene. For experimental purposes, a container is limited to containing one object at a time. The third experiment asks the manipulator to move the spoon (*grasp*) onto the plate (*contain*) in the first phase. At a later time, i.e., the second phase, the manipulator is then asked to move the same spoon (*grasp*) and put it into the bowl (*contain*). In this case, the task series are related. The *state keeper* retains awareness of the spoon’s location within the containers. The fourth experiment involves two *grasp*-able objects and two *contain*-able objects in a scene. It is an extension of the first two experiments, except now there are two objects and two containers. The task series consists of two tasks loosely related by virtue of affordances. In the first phase, one object is chosen to be placed into an empty container with the container randomly chosen and specified. In the second phase, the second object is required to be placed into an empty container. The state memory ensures that the second object is placed into the empty container.

Methodology and Evaluation

This subsection describes the different metrics of a successful trial for the five experiment classes. For each experiment in a class, we conduct 10 trials, and record the outcome as a *success* or a *failure*. A final score for each experiment is the number of successful trials for each experiment. Details are provided below.

Success in Each Scenario. The first three scenarios (seen categories, multiple objects, unseen categories) involve simple movements with three common affordances, including *grasp*, *contain* and *support*. Success for *grasp* requires the manipulator to stably grasp the target without dropping it. Success for *contain* requires the manipulator to put a small cuboid into a target container. Success for *support* requires the manipulator to put the small cuboid onto a target supportable surface without it falling off. For each trial, the target is randomly placed (position and orientation) in a visible and reachable area.

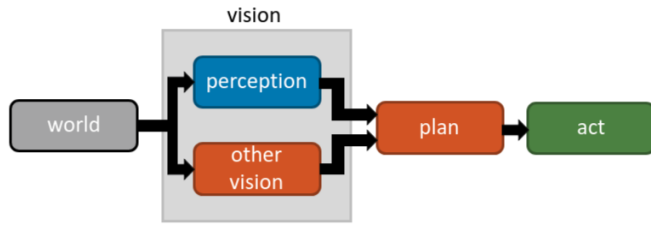


Figure 12. Illustration of the physical manipulation process. The vision includes the affordance detection (perception) and other vision processing functions. The visual results are then sent to the planning module followed by physical execution of our robotic manipulator (act module).

For the fourth scenario involving task-oriented tasks, a successful *pound peg into slot* trial requires the manipulator to first grasp the target without dropping it, and then fully pound the peg into the slot. A successful *cut through string* trial requires the manipulator to first grasp the target tool without dropping it, and then fully cut the string with the target.

For the last experiment set involving the modified PDDL, a successful trial requires the execution result to agree with the specified final state (one of the four commands discussed). For instance, if the predefined final state is *put knife into bowl*, success means the knife is inside the bowl, which requires the manipulator to grasp the knife and place it into the bowl.

Failure Categories. To properly evaluate and understand failure sources for the manipulation experiments, failures are divided into one of the three consecutive modules as shown in Fig. 12. With reference to the block diagram, the vision sensor provides visual input to the vision module. Within the vision module, two forms of processing occur. The first is affordance segmentation, here denoted by the *Perception* block. The second is additional visual processing to extract key geometric information for manipulation planning (3D locations, regions, or $SE(3)$ poses). The extracted signals are passed onto the planner (*Plan* block), which uses them to determine the world state and plan an action sequence to reach the target terminal world state. The action sequence gets executed in open-loop, e.g., there is no further visual processing to replan in the case of errors. The manipulator has one shot to complete the task (*Act* block).

Failures can occur in any of these modules. They are broken down into three categories: *perception*, *planning*, and *action*. Affordance related errors are counted towards the *perception* category. To separate the affordance detection error from general vision failures, the visual processing errors that result in bad plans will be counted towards the *planning* category. Additionally, if the planning system generates a bad plan from good information or fails to return a valid plan, the failure counts towards *planning*. Lastly, failures caused by bad physical movements leading to incomplete tasks are recorded as *action* failures.

Common Failure Modes. To simplify the analysis of results, this section describes the failure modes observed across all of the experiments. Several of the experiment scenarios exhibited the same failure modes, thus it is best to describe them in advance. For the affordance or *perception* failure mode, the error sources come in two types: direct

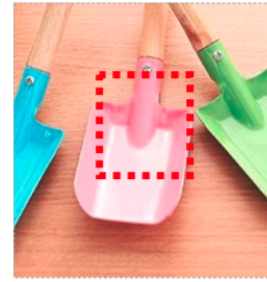


Figure 13. Illustration of the non-flat surface of the shovel. The dashed red box indicated the non-flat part inside the supportable area.

and indirect. A direct error is when the affordance prediction is incorrect and fails to identify the target affordance in the scene. Typically, the incorrect affordance is assigned to the region and the target affordance does not appear anywhere. A less common error is the failure to detect the object as an object via the *objectness* classifier, leading to no affordance predictions. In both cases the affordance is not recognized in the scene, and no planning nor manipulation actions can be taken. An indirect error is due to poor or noisy affordance segmentation. The bad segmentation negatively impacts the subsequent geometric reasoning in the other vision processes and leads to an incorrect plan. As a consequence, the manipulator will fail to complete the task (be it *grasp*, *contain*, *support*, *cut*, *pound*, or *scoop*).

Moving to the vision side of the *planning* errors, failures include incorrect height or length estimation due to depth image noise or bad relative geometry due to incorrect Aruco tag pose estimates. The other source of *planning* error occurs when the motion planner fails to generate a feasible plan (it happened once). The *action* failure modes include dropping the object while manipulator is moving, shifting of objects within the gripper while being manipulated, or colliding with objects while moving. Though collision could be a function of poor planning, it was common to have this occur once or twice for an experiment indicating that execution uncertainty or variance is the main factor. In-grasp shifts or drops cannot be corrected since there is no continual perception processing to ensure nothing of significance changes during open-loop execution. Larger grasping forces and closed-loop execution would improve on this failure type.

In several cases, the *action* failure is a function of the object geometry. Both the turners and the shovels do not lie flat on the surface nor have trivial geometry (see Fig. 13). Under normal circumstances a second arm would manipulate the object to present a better relative geometry for placing the object within the affordance action region. Or more tailored placement algorithms could be programmed for these surfaces. In the absence of a second arm or a custom place routine, the robot simply attempts to place the object onto the surface. For the turners and the shovels, the object being placed (a cuboid) sometimes slid or tumbled off of the surface. Since this investigation does not consider the physics nor dynamics of the manipulation actions, no modifications were made to correct for this failure mode. When describing these errors in the experiments, the abbreviated description of sliding or tumbling from the target object will be provided.

Table 5. Manipulation on Seen Categories

Object	DeepGrasp			AffNet			AffContext			similar	affordance
	Perc.	Plan	Act	Perc.	Plan	Act	Perc.	Plan	Act		
knife	10	10	10	10	10	10	10	10	10	yes	grasp
spoon	10	10	10	10	10	10	10	10	10	yes	grasp
mug	–	–	–	10	10	10	10	10	9	yes	contain
cup	–	–	–	10	10	10	9	9	8	yes	contain
turner	–	–	–	9	9	7	9	9	8	yes	support
shovel	–	–	–	8	8	6	8	8	7	yes	support
knife	10	10	10	10	10	10	10	10	10	no	grasp
spoon	10	10	10	10	10	10	10	10	10	no	grasp
mug	–	–	–	10	10	10	10	10	10	no	contain
cup	–	–	–	10	10	10	10	10	10	no	contain
turner	–	–	–	10	10	9	9	9	8	no	support
shovel	–	–	–	10	10	9	10	10	9	no	support
grasp average	10	10	10	10	10	10	10	10	10		
similar average	3.3	3.3	3.3	9.5	9.5	8.8	9.3	9.3	8.7		
all average	3.3	3.3	3.3	9.8	9.8	9.3	9.6	9.6	9.1		

Manipulation Results and Discussion

This section presents the experiment outcomes, discusses relative performance properties, and attempts to synthesize the overall findings associated to the experiments. Though the experiments attempt to quantify how well the affordance predictions translate to task-based manipulation, the tables will mark in bold the affordance *perception* outcomes for ease of identification. Based on the failure categories discussed earlier the *planning* and *action* outcomes will also be quantified. They will be in standard font in the same rows and to the right of the bold font *perception* values.

Affordance on Seen Categories

The proposed method is deployed and compared with state-of-the-art grasp (Chu et al. 2018) (*DeepGrasp*) and affordance (Do et al. 2018) (*AffNet*) detectors, with the results provided in Table 5. The *grasp average* row indicates perfect processing and execution for all three methods. The affordance recognition methods successfully identified the graspable regions and used them to lift the objects, thereby matching the performance of the specialized grasp recognition implementation. Moving to the *contain* affordance, the *AffNet* object-aware implementation had perfect visual processing and execution. In contrast *AffContext* experienced a single affordance recognition failure, and two execution failures. A similar trend in the performance loss occurs for the *support* affordance, whereby *AffNet* had 3 affordance failures and 6 subsequent execution failures while *AffContext* had 4 affordance failures and 4 subsequent execution failures. Affordance recognition for *AffContext* demonstrates a less than 3% performance drop over *AffNet* for affordance recognition and execution. These outcomes indicate that the affordance segmentation performance difference between the two methods, when applied to objects known by *AffNet*, does not influence task outcomes as much as the relative F-measures would indicate. For the image-split *AffNet* achieves a 0.80 weighted F-measure, while for the category-split *AffContext* achieves a 0.69 weighted F-measure, which reflects a 13.8% drop relative to *AffNet*.

For the *perception* failures of *AffNet*, 2 were direct (shovel) and 1 was indirect (turner). For *action* failures, all 6 were due to sliding or tumbling (turner or shovel). For *perception* failures of *AffContext*, 2 failures were direct (shovel) and 3 failures were indirect (cup and turner). For *action* failure, 2 failure were due to the end-effector accidentally hitting the containers (cups and mugs) and 4 failures were due to sliding or tumbling (turners and shovels). The main difference lies in the indirect affordance perception failure mode.

Affordance with Multiple Objects

The grasp detector, *DeepGrasp*, used for grasping comparisons is designed to predict multiple grasps on multiple objects in a scene. On account of this design, grasp selection can be augmented to require choosing a desired grasp from the candidate list (or subset thereof) or to require specifying a region of interest from which the top intersection grasp candidate must be chosen. This experiment adopts the latter modification (and thereby represents non-autonomous operation). The same affordances as in the previous experiment are evaluated: *grasp*, *contain* and *support*. The experimental results are reported in Table 6. For *grasp*, all three methods achieve perfect perception, planning, and execution. Given that *AffNet* was perfect across the other affordances, the discussion looks at them in aggregate. There was a single indirect *perception* failure for *AffContext* for the shovel (*support*). Lastly *AffNet* and *AffContext* had 2 and 3 execution failures, respectively, for a differential of 1. The 2 *action* failures in *AffNet* were due to sliding/tumbling (turner). Likewise, the 3 *action* failures in *AffContext* were due to sliding/tumbling (turner). Overall, *AffContext* shows a less than 2% affordance perception difference and a less than 2% execution difference (for an overall less than 4% task completion difference).

Affordance on Unseen Categories

Given that *AffNet* depends on the object prior and is limited to the training categories, it will not be capable of recognizing affordances for novel objects. Thus, even though it was run for this scenario, the algorithm did not detect the presented objects and could therefore not

Table 6. Manipulation with Multiple Objects in Scene

Object	DeepGrasp			AffNet			AffContext			affordance
	Perc.	Plan	Act	Perc.	Plan	Act	Perc.	Plan	Act	
knife	10	10	10	10	10	10	10	10	10	grasp
spoon	10	10	10	10	10	10	10	10	10	grasp
mug	–	–	–	10	10	10	10	10	10	contain
cup	–	–	–	10	10	10	10	10	10	contain
turner	–	–	–	10	10	8	10	10	7	support
shovel	–	–	–	10	10	10	9	9	9	support
grasp average	10	10	10	10	10	10	10	10	10	
all average	3.3	3.3	3.3	10	10	9.7	9.8	9.8	9.3	

Table 7. Manipulation on Unseen Categories.

Object	DeepGrasp			AffNet			AffContext			Affordance
	Perc.	Plan	Act	Perc.	Plan	Act	Perc.	Plan	Act	
screwdriver	10	10	10	–	–	–	10	10	10	grasp
juice bottle	10	10	10	–	–	–	10	10	10	grasp
mouse	10	10	10	–	–	–	10	10	10	grasp
plate	–	–	–	–	–	–	10	10	10	contain
jar	–	–	–	–	–	–	9	8	8	contain
can	–	–	–	–	–	–	10	10	10	contain
griddle turner	–	–	–	–	–	–	10	10	8	support
grill spatula	–	–	–	–	–	–	10	10	9	support
pie server	–	–	–	–	–	–	9	9	9	support
grasp average	10	10	10	0	0	0	10	10	10	
all average	3.3	3.3	3.3	0	0	0	9.8	9.7	9.3	

recognize any affordances. In what follows *AffNet* will not be referenced since all tests failed. *DeepGrasp* is not restricted to specific object categories and can recognize graspable regions of objects. Table 7 reports the outcomes for this unseen categories experiment. Again, the *grasp* affordance was perfectly perceived and executed for *AffContext*. The *contain* and *support* affordances had 1 error each (out of 30 trials per affordance class) for a 3% affordance recognition error rate. These errors were indirect affordance perception errors. When moving from the affordance perception to planning, then to action, there was a total of 4 additional failures to complete the task. The 1 *planning* failure was due to incorrect height estimation (jar). The 3 *action* failures were sliding/tumbling errors (turner and spatula).

Though there is a performance loss relative to *AffNet* for seen objects, the ability to operate without explicit object labels permits more general operation of *AffContext*. In fact, affordance prediction for these unseen objects matched *AffNet* for the seen objects. The consistent task performance for these cases relative to the earlier seen category tests (Tables 5 & 6), indicates good affordance generalization performance for *AffContext* to unseen objects with known affordance categories.

Affordance for Task-Oriented Grasping

These experiments move beyond *pick-and-place* types of affordance action tasks, which is what *grasp*, *contain* and *support* test. The affordances of *pound* and *cut* require grasping an object and using it to achieve a given goal for some other object in the world. In this case, the other object has a known action region relative to an Aruco tag. Table 8 reports the results from these experiments, which involve seen and unseen objects.

For the seen objects *AffNet* and *AffContext* had the same affordance perception performance, however *AffContext* had one more planning failure than *AffNet* (3 vs 2). The *planning* failures in all cases were due to visual processing errors (bad heights). Compared to previous scenarios, the two designed task-oriented grasp tasks in this scenario require good estimation of the heights of the peg and the string. Apart from the Aruco tag in the work space for estimating relative transformation between camera and manipulator, another Aruco tag is attached to the top surface of the box with the peg or string as shown in Fig. 10. Due to the measurement uncertainty from the depth image and the Aruco tags pose estimates, the returned height estimates for the *pound* or *cut* position are sometimes not accurate enough and led to misses. The *action* failure for *AffNet* was due to the hammer tilting after being grasped.

Moving to the unseen objects, the self-made tenderizer, see Fig. 10(c), case had an indirect *perception* failure for the *grasp* affordance plus a *planning* failure (bad height). For the letter opener (see Fig. 10(d)), there was one direct *perception* failure for the *grasp* affordance and an *action* failure. The letter opener tilted after the first cut attempt so that the two additional attempts could not succeed.

The affordance recognition for *AffContext* in this set of experiments is close to that of the earlier experiments but slightly worse. There is a 5% error rate at the affordance level with a further 12% drop when translating to action. This increased performance drop from perception to action is a function of more perception-based measurements outside of the affordance category. They accounted for 4 of the 5 post-*perception* module failures, or 80%. In contrast the earlier experiments have an aggregate *planning* failure rate ten times lower, at 8%. The current processing schemes are not robust to non-affordance visual processing errors. Nevertheless,

Table 8. Task-Oriented Grasping and Manipulation

Object	AffNet			AffContext			Affordance
	Perc.	Plan	Act	Perc.	Plan	Act	
hammer	10	9	8	10	8	8	grasp, pound
tenderizer	–	–	–	9	8	8	grasp, pound
knife	10	9	9	10	9	9	grasp, cut
letter opener	–	–	–	9	9	8	grasp, cut
seen average	10	9.0	8.5	10	8.5	8.5	
all average	5.0	4.5	4.3	9.5	8.5	8.3	

Table 9. Manipulation with Object Detector and State-PDDL.

Activity	Success			Affordance	Detection	State
	Perc.	Plan	Act			
pick knife or spoon into bowl	10	10	10	grasp, contain	✓	
select trowel or spoon to scoop beans	10	10	8	grasp, scoop, contain	✓	
grasp spoon to plate then move to bowl	8	7	7	grasp, contain	✓	✓
place objects into empty containers	9	8	8	grasp, contain	✓	✓
average	9.3	8.8	8.3			

these results demonstrate the power of combining affordance reasoning with symbolic reasoning to plan and execute manipulation activities.

Affordance with Modified PDDL Pipeline

Including state memory of prior actions to support contemporary vision failures associated to overlapping or occluding objects supports additional experiments that have goal state specification with multiple, feasible solution plans. The experiments led to the outcomes reported in Table 9. For the first two experiments, the *perception* component was perfect with only *action* failures affecting task completions. The 2 *action* failures were due to hitting the edge of the bowl while performing the *scoop* action primitive.

The third and fourth experiments require the state memory component to complete the specified task. During successful operation for the third experiment, the system correctly identifies the empty container with the *state keeper* as well as where the object of interest is placed on the container (e.g. the *plate*). The 2 *perception* failures for the third experiment, *grasp spoon to plate then move to bowl*, were direct and caused by the *objectness* of the plate not being detected by the affordance detector. The 1 *action* failure was a motion planning failure. For the fourth experiment, *place objects into empty containers*, the system keeps track of the state of each container in order to accept different combinations of the goal state. The 1 *perception* failure was direct; the system did not perceive the *contain* affordance for the mug. The 1 *planning* failure was due to the mug not being detected on the object detector side (it is not an affordance related error). The *perception* error rate for this set of experiments (~7%) is a bit higher than for the previous ones in aggregate (~3%), which reflects the repeated use of the affordance predictions as part of a sequential task. Meanwhile, the execution success rate drop of 10% is consistent with the previous task-oriented experiments. This experiment set demonstrates that the *AffContext* perception module and PDDL planning module provides the flexibility to specify and execute goal-oriented manipulation tasks based on affordance informed state awareness of the world.

Discussion of Affordances and Manipulation

Overall performance is around 97% correct affordance recognition in simple scenarios (seen categories, multiple objects, unseen categories), with a 92% task completion success rate. The 3% drop in affordance recognition could be improved through better network design with regards to the overall detection and recognition processes, while the subsequent 5% performance drop could be improved through better segmentation (more consistent regions) and improved awareness of the scene geometry (e.g., orientation of support surfaces). Since the neural network model in the physical experiment is trained on the UMD dataset, domain shift between training dataset and workspace may be a source of performance loss. Though we showed that perfect estimation of the affordance map is not a requirement for success in execution, better affordance segmentation could be achieved by reducing the domain shift. A simple solution involves finetuning on a small set of workspace or task-relevant training data before deployment.

In addition to simple manipulation tasks with affordance-based pick-and-place action demands, the task-oriented manipulation or sequential manipulation experiments reflects moderately complex scenarios requiring additional geometric processing to follow through on the task by exploiting a part affordance. Affordance perception for these demonstrated a 94% success rate with *AffContext* when aggregated, while execution led to a final success rate of 83% (for an 11% drop from perception to action). The larger drop is mostly a function of errors in the additional visual reasoning modules. The *perception* and *action* outcomes are in agreement with the simpler experiment given that these task-oriented experiments involve sequential use of affordances to meet the task objective.

Aggregating all experiments, affordance recognition performance is 96% and task completion is 88%. Our earlier work has collected grasping success rates for various deep learning algorithms (see Chu et al. (2018) and Lin et al. (2020)). For *vision only* grasp detection, state-of-the-art success rates vary from 87% to 97%. As a source of *grasp* affordance information, the grasping success rate across the experiments is at the upper end of this range

and matches the best methods. Expanding further to include the additional affordance cases, the success rates of the affordance perception module continues to lie at the upper end of the vision-only success rates for published grasping pipelines. For *embodied grasping* based on published state-of-the-art grasping algorithms, success varies from 80% to 97% for the simple case of grasping. The success rates of the simple affordance-based manipulation tasks lie at the upper range of the embodied grasping range. Meanwhile, the success rates of the various, more involved manipulation activities lie at the lower end of this range. However, the performance drop is a function of errors in other parts of the perceive, plan, act pipeline. These outcomes can be improved through better implementations of the supporting perception and planning modules. Across the experiments, 6 of the 7 affordances in the UMD dataset were tested with the missing one being *wrap-grasp*. Considering the tasks involved, affordances employed, and the outcomes achieved, *AffContext* exhibits state-of-the-art performance for the affordance perception pipeline and successfully contributes towards a perception to action pipeline.

In robotics, affordances have long been hypothesized to be a rich and important source of action opportunities for seen objects. They can contribute to symbolic planning needs through their integration into a scene reasoning module. This paper designed a neural network that successfully linked visually derived affordance recognition outputs to physical manipulation plans. With affordance, robot agents with grasping abilities may go beyond simple pick-and-place tasks and pursue more general, goal-directed manipulations. The proposed pipeline demonstrated both simple manipulations and task-oriented manipulation activities.

Conclusion

This paper describes and evaluates an affordance-based scene reasoning pipeline for robotic manipulation. The core component enabling this is an object-agnostic affordance recognition neural network, *AffContext*, for predicting the affordances of object parts within an image. The deep network learns to generalize affordance segmentation across unseen object categories in support of robotic manipulation. In particular, a self-attention mechanism within the affordance segmentation branch selectively adapts to contextual dependencies within each instance region. Second, affordance category attributes guide the feature learning and compensate for the absence of object category priors. Evaluation of the *perception* pipeline with the UMD dataset used the novel category split for comparison to state-of-the-art methods, including several image-based and region-based baselines. Experiments with physical manipulation demonstrated the effectiveness of the proposed framework for manipulating unseen object categories in the real-world. It also demonstrated the successful integration of affordance recognition with symbolic reasoning and planning in support of goal-oriented manipulation. Future work aims to integrate affordance knowledge with scene graph knowledge to support more complex manipulation sequences. It will also seek to plan activities involving longer

sequences of atomic actions. All code and data will be publicly released.

Funding

This work was supported in part by NSF Award #1605228.

References

- Akbari A and Rosell J (2015) Ontological physics-based motion planning for manipulation. In: *IEEE Conference on Emerging Technologies and Factory Automation*. pp. 1–7.
- Akbari A and Rosell J (2016) Task planning using physics-based heuristics on manipulation actions. In: *IEEE International Conference on Emerging Technologies and Factory Automation*. pp. 1–8.
- Aldoma A, Tombari F and Vincze M (2012) Supervised learning of hidden and non-hidden 0-order affordances and detection in real scenes. In: *IEEE International Conference on Robotics and Automation*. pp. 1732–1739.
- Antanas L, Moreno P, Neumann M, de Figueiredo RP, Kersting K, Santos-Victor J and De Raedt L (2019) Semantic and geometric reasoning for robotic grasping: a probabilistic logic approach. *Autonomous Robots* 43(6): 1393–1418.
- Bicchi A and Kumar V (2000) Robotic grasping and contact: A review. In: *IEEE International Conference on Robotics and Automation*. pp. 348–353.
- Bohg J, Morales A, Asfour T and Kragic D (2014) Data-driven grasp synthesis survey. *IEEE Transactions on Robotics* 30(2): 289–309.
- Cambon S, Gravot F and Alami R (2004) A robot task planner that merges symbolic and geometric reasoning. In: *European Conference on Artificial Intelligence*. pp. 895–899.
- Chen L, Nugent C and Okeyo G (2013) An ontology-based hybrid approach to activity modeling for smart homes. *IEEE Transactions on Human-Machine Systems* 44(1): 92–105.
- Chen LC, Papandreou G, Kokkinos I, Murphy K and Yuille AL (2018) Deeplab: Semantic image segmentation with deep convolutional nets, atrous convolution, and fully connected crfs. *IEEE Transactions on Pattern Analysis and Machine Intelligence* 40(4): 834–848.
- Chen LC, Papandreou G, Schroff F and Adam H (2017) Rethinking atrous convolution for semantic image segmentation. *arXiv preprint arXiv:1706.05587*.
- Cheng HT, Sun FT, Griss M, Davis P, Li J and You D (2013) Nuactiv: Recognizing unseen new activities using semantic attribute-based learning. In: *International Conference on Mobile Systems, Applications, and Services*. ACM, pp. 361–374.
- Chu FJ, Xu R, Seguin L and Vela PA (2019a) Toward affordance detection and ranking on novel objects for real-world robotic manipulation. *IEEE Robotics and Automation Letters* 4(4): 4070–4077.
- Chu FJ, Xu R and Vela PA (2018) Real-world multiobject, multigrasp detection. *IEEE Robotics and Automation Letters* 3(4): 3355–3362.
- Chu FJ, Xu R and Vela PA (2019b) Learning affordance segmentation for real-world robotic manipulation via synthetic images. *IEEE Robotics and Automation Letters* 4(2): 1140–1147.

- Cordts M, Omran M, Ramos S, Rehfeld T, Enzweiler M, Benenson R, Franke U, Roth S and Schiele B (2016) The cityscapes dataset for semantic urban scene understanding. In: *IEEE Conference on Computer Vision and Pattern Recognition*. pp. 3213–3223.
- de Silva L, Pandey AK, Gharbi M and Alami R (2013) Towards combining htn planning and geometric task planning. *RSS Workshop on Combined Robot Motion Planning and AI Planning for Practical Applications*.
- Dehban A, Jamone L, Kampff AR and Santos-Victor J (2016) Denoising auto-encoders for learning of objects and tools affordances in continuous space. In: *IEEE International Conference on Robotics and Automation*. pp. 4866–4871.
- Deng J, Dong W, Socher R, Li LJ, Li K and Fei-Fei L (2009) Imagenet: A large-scale hierarchical image database. In: *IEEE Conference on Computer Vision and Pattern Recognition*. pp. 248–255.
- Ding H, Jiang X, Shuai B, Qun Liu A and Wang G (2018) Context contrasted feature and gated multi-scale aggregation for scene segmentation. In: *IEEE Conference on Computer Vision and Pattern Recognition*. pp. 2393–2402.
- Do TT, Nguyen A and Reid I (2018) AffordanceNet: An end-to-end deep learning approach for object affordance detection. In: *IEEE International Conference on Robotics and Automation*. pp. 1–5.
- Duan K, Parikh D, Crandall D and Grauman K (2012) Discovering localized attributes for fine-grained recognition. In: *IEEE Conference on Computer Vision and Pattern Recognition*. pp. 3474–3481.
- Erdem E, Haspalamutgil K, Palaz C, Patoglu V and Uras T (2011) Combining high-level causal reasoning with low-level geometric reasoning and motion planning for robotic manipulation. In: *IEEE International Conference on Robotics and Automation*. pp. 4575–4581.
- Farhadi A, Endres I, Hoiem D and Forsyth D (2009) Describing objects by their attributes. In: *IEEE Conference on Computer Vision and Pattern Recognition*. pp. 1778–1785.
- Fikes RE and Nilsson NJ (1971) Strips: A new approach to the application of theorem proving to problem solving. *Artificial intelligence* 2(3-4): 189–208.
- Florence PR, Manuelli L and Tedrake R (2018) Dense object nets: Learning dense visual object descriptors by and for robotic manipulation. In: *Conference on Robot Learning*. pp. 373–385.
- Fu J, Liu J, Tian H, Li Y, Bao Y, Fang Z and Lu H (2019) Dual attention network for scene segmentation. In: *IEEE Conference on Computer Vision and Pattern Recognition*. pp. 3146–3154.
- Gaschler A, Kessler I, Petrick RP and Knoll A (2015) Extending the knowledge of volumes approach to robot task planning with efficient geometric predicates. In: *IEEE International Conference on Robotics and Automation*. pp. 3061–3066.
- Ghallab M, Nau D and Traverso P (2004) *Automated Planning: theory and practice*. Elsevier.
- Gravot F, Haneda A, Okada K and Inaba M (2006) Cooking for humanoid robot, a task that needs symbolic and geometric reasonings. In: *IEEE International Conference on Robotics and Automation*. pp. 462–467.
- Guo D, Sun F, Liu H, Kong T, Fang B and Xi N (2017) A hybrid deep architecture for robotic grasp detection. In: *IEEE International Conference on Robotics and Automation*. pp. 1609–1614.
- He K, Gkioxari G, Dollár P and Girshick R (2017) Mask r-cnn. In: *IEEE International Conference on Computer Vision*. pp. 2980–2988.
- Helmert M (2006) The fast downward planning system. *Journal of Artificial Intelligence Research* 26: 191–246.
- Jaderberg M, Mnih V, Czarnecki WM, Schaul T, Leibo JZ, Silver D and Kavukcuoglu K (2017) Reinforcement learning with unsupervised auxiliary tasks. In: *International Conference on Learning Representations*.
- Kaelbling LP and Lozano-Pérez T (2011) Hierarchical task and motion planning in the now. In: *IEEE International Conference on Robotics and Automation*. pp. 1470–1477.
- Kalashnikov D, Irpan A, Pastor P, Ibarz J, Herzog A, Jang E, Quillen D, Holly E, Kalakrishnan M, Vanhoucke V and Levine S (2018) QT-Opt: Scalable deep reinforcement learning for vision-based robotic manipulation. In: *Conference on Robot Learning*. pp. 651–673.
- Krasin I, Duerig T, Alldrin N, Veit A, Abu-El-Haija S, Belongie S, Cai D, Feng Z, Ferrari V, Gomes V, Gupta A, Narayanan D, Sun C, Chechik G and Murphy K (2016) Openimages: A public dataset for large-scale multi-label and multi-class image classification. *Dataset available from <https://github.com/openimages>*.
- Krizhevsky A (2009) Learning multiple layers of features from tiny images. Technical report, Citeseer.
- Krizhevsky A, Sutskever I and Hinton GE (2012) Imagenet classification with deep convolutional neural networks. In: *Advances in Neural Information Processing Systems*. pp. 1097–1105.
- Kumar N, Berg A, Belhumeur PN and Nayar S (2011) Describable visual attributes for face verification and image search. *IEEE Transactions on Pattern Analysis and Machine Intelligence* 33(10): 1962–1977.
- Kumar N, Berg AC, Belhumeur PN and Nayar SK (2009) Attribute and simile classifiers for face verification. In: *IEEE International Conference on Computer Vision*. pp. 365–372.
- Lab RL (2013) Cornell grasping dataset. http://pr.cs.cornell.edu/grasping/rect_data/data.php. Accessed: 2019-09-01.
- Lenz I, Lee H and Saxena A (2015) Deep learning for detecting robotic grasps. *The International Journal of Robotics Research* 34(4-5): 705–724.
- Levihn M and Stilman M (2014) Using environment objects as tools: Unconventional door opening. In: *IEEE/RSJ International Conference on Intelligent Robots and Systems*. pp. 2502–2508.
- Levine S, Pastor P, Krizhevsky A and Quillen D (2016) Learning hand-eye coordination for robotic grasping with large-scale data collection. In: *International Symposium on Experimental Robotics*. pp. 173–184.
- Li LJ, Su H, Lim Y and Fei-Fei L (2010) Objects as attributes for scene classification. In: *European Conference on Computer Vision*. Springer, pp. 57–69.
- Li Y (2017) Deep reinforcement learning: An overview. *arXiv preprint arXiv:1701.07274*.
- Lin Y, Tang C, Chu FJ and Vela PA (2020) Using Synthetic Data and Deep Networks to Recognize Primitive Shapes for Object Grasping. *IEEE International Conference on Robotics and Automation*.

- Liu Z, Chen D, Wurm KM and von Wichert G (2020) Table-top scene analysis using knowledge-supervised mcmc. *arXiv preprint arXiv:2002.08417*.
- Liu Z, Luo P, Qiu S, Wang X and Tang X (2016) Deepfashion: Powering robust clothes recognition and retrieval with rich annotations. In: *IEEE Conference on Computer Vision and Pattern Recognition*. pp. 1096–1104.
- Margolin R, Zelnik-Manor L and Tal A (2014) How to evaluate foreground maps? In: *IEEE Conference on Computer Vision and Pattern Recognition*. pp. 248–255.
- Marthi B, Russell SJ and Wolfe JA (2007) Angelic semantics for high-level actions. In: *International Conference on Automated Planning and Scheduling*. pp. 232–239.
- McDermott D, Ghallab M, Howe A, Knoblock C, Ram A, Veloso M, Weld D and Wilkins D (1998) PDDL—the planning domain definition language.
- Migimatsu T and Bohg J (2020) Object-centric task and motion planning in dynamic environments. *IEEE Robotics and Automation Letters* 5(2): 844–851.
- Myers A, Teo CL, Fermüller C and Aloimonos Y (2015) Affordance detection of tool parts from geometric features. In: *IEEE International Conference on Robotics and Automation*. pp. 1374–1381.
- Ngiam J, Khosla A, Kim M, Nam J, Lee H and Ng AY (2011) Multimodal deep learning. In: *International Conference on Machine Learning*. ACM, pp. 689–696.
- Nguyen A, Kanoulas D, Caldwell DG and Tsagarakis NG (2016a) Detecting object affordances with convolutional neural networks. In: *IEEE/RSJ International Conference on Intelligent Robots and Systems*. pp. 2765–2770.
- Nguyen A, Kanoulas D, Caldwell DG and Tsagarakis NG (2016b) Preparatory object reorientation for task-oriented grasping. In: *IEEE/RSJ International Conference on Intelligent Robots and Systems*. pp. 893–899.
- Nguyen A, Kanoulas D, Caldwell DG and Tsagarakis NG (2017) Object-based affordances detection with convolutional neural networks and dense conditional random fields. In: *IEEE/RSJ International Conference on Intelligent Robots and Systems*. pp. 5908–5915.
- Pandey AK, Saut JP, Sidobre D and Alami R (2012) Towards planning human-robot interactive manipulation tasks: Task dependent and human oriented autonomous selection of grasp and placement. In: *IEEE RAS and EMBS International Conference on Biomedical Robotics and Biomechatronics*. pp. 1371–1376.
- Pednault EP (1994) Adl and the state-transition model of action. *Journal of logic and computation* 4(5): 467–512.
- Plaku E and Hager GD (2010) Sampling-based motion and symbolic action planning with geometric and differential constraints. In: *IEEE International Conference on Robotics and Automation*. pp. 5002–5008.
- Redmon J and Angelova A (2015) Real-time grasp detection using convolutional neural networks. In: *IEEE International Conference on Robotics and Automation*. pp. 1316–1322.
- Ren S, He K, Girshick R and Sun J (2015) Faster R-CNN: Towards real-time object detection with region proposal networks. In: *Advances in Neural Information Processing Systems*. pp. 91–99.
- Rezapour Lakani S, Rodríguez-Sánchez AJ and Piater J (2019) Towards affordance detection for robot manipulation using affordance for parts and parts for affordance. *Autonomous Robots* 43(5): 1155–1172.
- Richter SR, Vineet V, Roth S and Koltun V (2016) Playing for data: Ground truth from computer games. In: *European Conference on Computer Vision*. Springer, pp. 102–118.
- Ros G, Sellart L, Materzynska J, Vazquez D and Lopez AM (2016) The synthia dataset: A large collection of synthetic images for semantic segmentation of urban scenes. In: *IEEE Conference on Computer Vision and Pattern Recognition*. pp. 3234–3243.
- Roy A and Todorovic S (2016) A multi-scale cnn for affordance segmentation in rgb images. In: *European Conference on Computer Vision*. Springer, pp. 186–201.
- Sawatzky J and Gall J (2017) Adaptive binarization for weakly supervised affordance segmentation. In: *IEEE International Conference on Computer Vision Workshops*. pp. 1383–1391.
- Sawatzky J, Srikantha A and Gall J (2017) Weakly supervised affordance detection. In: *IEEE Conference on Computer Vision and Pattern Recognition*. pp. 5197–5206.
- Saxena A, Driemeyer J and Ng AY (2008) Robotic grasping of novel objects using vision. *The International Journal of Robotics Research* 27(2): 157–173.
- Shimoga KB (1996) Robot grasp synthesis algorithms: A survey. *The International Journal of Robotics Research* 15(3): 230–266.
- Simonyan K and Zisserman A (2015) Very deep convolutional networks for large-scale image recognition. In: *International Conference on Learning Representations*.
- Srikantha A and Gall J (2016) Weakly supervised learning of affordances. *arXiv preprint arXiv:1605.02964*.
- Srivastava S, Fang E, Riano L, Chitnis R, Russell S and Abbeel P (2014) Combined task and motion planning through an extensible planner-independent interface layer. In: *IEEE International Conference on Robotics and Automation*. pp. 639–646.
- Stilman M and Kuffner JJ (2005) Navigation among movable obstacles: Real-time reasoning in complex environments. *International Journal of Humanoid Robotics* 2(04): 479–503.
- Suárez-Hernández A, Alenyà G and Torras C (2018) Interleaving hierarchical task planning and motion constraint testing for dual-arm manipulation. In: *IEEE/RSJ International Conference on Intelligent Robots and Systems*. pp. 4061–4066.
- Sui Z, Xiang L, Jenkins OC and Desingh K (2017) Goal-directed robot manipulation through axiomatic scene estimation. *The International Journal of Robotics Research* 36(1): 86–104.
- Sun Y, Bo L and Fox D (2013) Attribute based object identification. In: *IEEE International Conference on Robotics and Automation*. pp. 2096–2103.
- Tenorth M and Beetz M (2009) Knowrobknowledge processing for autonomous personal robots. In: *IEEE/RSJ International Conference on Intelligent Robots and Systems*. pp. 4261–4266.
- Toussaint M, Plath N, Lang T and Jetchev N (2010) Integrated motor control, planning, grasping and high-level reasoning in a blocks world using probabilistic inference. In: *IEEE International Conference on Robotics and Automation*. pp. 385–391.
- Ugur E and Piater J (2015) Bottom-up learning of object categories, action effects and logical rules: From continuous manipulative exploration to symbolic planning. In: *IEEE International Conference on Robotics and Automation*. pp. 2627–2633.

- Vaswani A, Shazeer N, Parmar N, Uszkoreit J, Jones L, Gomez AN, Kaiser Ł and Polosukhin I (2017) Attention is all you need. In: *Advances in Neural Information Processing Systems*. pp. 5998–6008.
- Winkler J, Bartels G, Mösenlechner L and Beetz M (2012) Knowledge enabled high-level task abstraction and execution. In: *Conference on Advances in Cognitive Systems*, volume 2. Citeseer, pp. 131–148.
- Yang Y, Li Y, Fermuller C and Aloimonos Y (2015) Robot learning manipulation action plans by” watching” unconstrained videos from the world wide web. In: *AAAI Conference on Artificial Intelligence*.
- Yuan Y and Wang J (2018) Ocnet: Object context network for scene parsing. *arXiv preprint arXiv:1809.00916* .
- Zeng A, Song S, Welker S, Lee J, Rodriguez A and Funkhouser T (2018a) Learning synergies between pushing and grasping with self-supervised deep reinforcement learning. In: *IEEE/RSJ International Conference on Intelligent Robots and Systems*. pp. 4238–4245.
- Zeng Z, Zhou Z, Sui Z and Jenkins OC (2018b) Semantic robot programming for goal-directed manipulation in cluttered scenes. In: *IEEE International Conference on Robotics and Automation*. pp. 7462–7469.
- Zhang H, Dana K, Shi J, Zhang Z, Wang X, Tyagi A and Agrawal A (2018) Context encoding for semantic segmentation. In: *IEEE Conference on Computer Vision and Pattern Recognition*. pp. 7151–7160.
- Zhang Z, Luo P, Loy CC and Tang X (2015) Learning deep representation for face alignment with auxiliary attributes. *IEEE Transactions on Pattern Analysis and Machine Intelligence* 38(5): 918–930.
- Zhao H, Shi J, Qi X, Wang X and Jia J (2017) Pyramid scene parsing network. In: *IEEE Conference on Computer Vision and Pattern Recognition*. pp. 2881–2890.